Available online at www.sciencedirect.com
SCIENCE DIRECT®
Coordination Chemistry Reviews 250 (2006) 900–910
COORDINATION CHEMISTRY REVIEWS
www.elsevier.com/locate/ccr

Review

Relativistic energy-consistent ab initio pseudopotentials as tools for quantum chemical investigations of actinide systems

Xiaoyan Cao, Michael Dolg*

Institute for Theoretical Chemistry, University of Cologne, Greinstr. 4, D-50939 Cologne, Germany

Received 21 September 2005; accepted 6 January 2006
Available online 3 March 2006

Contents

1. Introduction 900
   1.1. Relativistic and correlation effects in actinides 901
   1.2. Effective core potentials 903
2. Energy-consistent pseudopotentials 904
   2.1. Valence-only model Hamiltonian 904
   2.2. Choice of the core 905
   2.3. Pseudopotential parameter adjustment 906
   2.4. Optimization of valence basis sets 906
3. Calibration calculations 906
   3.1. Atomic ionization potentials and excitation energies 906
   3.2. Diatomic molecules 907
4. Selected applications 907
5. Outlook 907
6. Conclusions 909
   Acknowledgements 909
   References 909

Abstract

The method of relativistic energy-consistent ab initio pseudopotentials is briefly reviewed, paying special attention to the parametrization for actinide elements and the optimization of corresponding valence basis sets. Based on atomic frozen-core data it is argued that only a small-core approach is sufficiently accurate. Calibration calculations for atoms and diatomic molecules are briefly described and an overview is given over recent applications of the method to larger actinide systems. Shortcommings of the currently applied approach are discussed and future developments, towards higher accuracy as well as towards a simplified treatment of actinides in quantum chemical calculations, are outlined.

Keywords: Pseudopotentials; Actinides; Relativistic effects; Electronic structure; Calculation

1. Introduction

The application of modern first-principles electronic structure theory to molecules containing actinide elements is still a tremendous challenge. Large relativistic effects, including usually non-negligible effects of spin–orbit interaction, as well as significant and often hard to calculate correlation contributions are the main obstacles to accurate investigations. In addition, lack of experimental data makes systematic calibration studies of computational models very difficult. Nevertheless, due to methodological development in relativistic electronic structure theory as well as the beneficial progress in computer technology quantum chemical calculations on actinide compounds are about to become almost routine and their results provide a useful

* Corresponding author. Tel.: +49 2214706893; fax: +49 2214706896.
E-mail address: m.dolg@uni-koeln.de (M. Dolg).

0010-8545/$ – see front matter © 2006 Elsevier B.V. All rights reserved.
doi:10.1016/j.ccr.2006.01.003

Table 1
Electronic ground configurations and states of the actinides An^{n+} ($n = 0$–4) [17]

$_Z$An	M		M^{1+}		M^{2+}		M^{3+}		M^{4+}	
$_{89}$Ac	d^1s^2	$^2D_{3/2}$	s^2	$^1S_0$	s^1	$^2S_{1/2}$		$^1S_0$	p^5	$^2P_{3/2}$
$_{90}$Th	d^2s^2	$^3F_2$	d^2s^1	$^4F_{3/2}$	f^1d^1	$^1G_4$	f^1	$^2F_{5/2}$	p^6	$^1S_0$
$_{91}$Pa	$f^2d^1s^2$	$^4K_{11/2}$	f^2s^2	$^3H_4$	f^2d^1	$^4I_{11/2}$	f^2	$^3H_4$	f^1	$^2F_{5/2}$
$_{92}$U	$f^3d^1s^2$	$^5K_6$	f^3s^2	$^4I_{9/2}$	f^4	$^5I_4$	f^3	$^4I_{9/2}$	f^2	$^3H_4$
$_{93}$Np	$f^4d^1s^2$	$^6L_{11/2}$	$f^4d^1s^1$	$^7L_5$	f^5	$^6H_{5/2}$	f^4	$^5I_4$	f^3	$^4I_{9/2}$
$_{94}$Pu	f^6s^2	$^7F_0$	f^6s^1	$^8F_{1/2}$	f^6	$^7F_0$	f^5	$^6H_{5/2}$	f^4	$^5I_4$
$_{95}$Am	f^7s^2	$^8S_{7/2}$	f^7s^1	$^9S_4$	f^7	$^8S_{7/2}$	f^6	$^7F_0$	f^5	$^6H_{5/2}$
$_{96}$Cm	$f^7d^1s^2$	$^9D_2$	f^7s^2	$^8S_{7/2}$	f^8	$^7F_6$	f^7	$^8S_{7/2}$	f^6	$^7F_0$
$_{97}$Bk	f^9s^2	$^6H_{15/2}$	f^9s^1	$^7H_8$	f^9	$^6H_{15/2}$	f^8	$^7F_6$	f^7	$^8S_{7/2}$
$_{98}$Cf	$f^{10}s^2$	$^5I_8$	$f^{10}s^1$	$^6I_{17/2}$	f^{10}	$^5I_8$	f^9	$^6H_{15/2}$	f^8	$^7F_6$
$_{99}$Es	$f^{11}s^2$	$^4I_{15/2}$	$f^{11}s^1$	$^5I_8$	f^{11}	$^4I_{15/2}$	f^{10}	$^5I_8$	f^9	$^6H_{15/2}$
$_{100}$Fm	$f^{12}s^2$	$^3H_6$	$f^{12}s^1$	$^4H_{13/2}$	f^{12}	$^3H_6$	f^{11}	$^4I_{15/2}$	f^{10}	$^5I_8$
$_{101}$Md	$f^{13}s^2$	$^2F_{7/2}$	$f^{13}s^1$	$^3F_4$	f^{13}	$^2F_{7/2}$	f^{12}	$^3H_6$	f^{11}	$^4I_{15/2}$
$_{102}$No	$f^{14}s^2$	$^1S_0$	$f^{14}s^1$	$^2S_{1/2}$	f^{14}	$^1S_0$	f^{13}	$^2F_{7/2}$	f^{12}	$^3H_6$
$_{103}$Lr	$f^{14}p^1s^2$	$^2P_{1/2}$	$f^{14}s^2$	$^1S_0$	$f^{14}s^1$	$^2S_{1/2}$	f^{14}	$^1S_0$	f^{13}	$^2F_{7/2}$

f, d and s denote the 5f, 6d and 7s shells. Calculations find a Pa^{2+} $^2H_{11/2}$ ground state [19].

source of information for experimentalists. In 1987, a brief review on relativistic electronic structure calculations on f element molecules by Pyykkö listed only 53 references for actinides, ranging from semiempirical valence-only (VO) approaches like extended Hückel theory to fully relativistic all-electron (AE) Dirac–Hartree–Fock (DHF) one-center-expansions [1]. Nowadays a similar number of studies appears in literature almost every year, many of them including relativistic effects and especially correlation effects in a much more rigorous manner. The present article does not intend to give a complete overview over all computational approaches used at present in actinide quantum chemical studies, but rather focuses on one approach which was quite successful during the last decade, i.e. relativistic energy-consistent small-core ab initio pseudopotentials (PPs) [2] and optimized valence basis sets [3,4] combined with wavefunction-based correlated ab initio methods or density functional theory (DFT) approaches. For alternative approaches and further references the reader is referred to a number of review articles on quantum chemistry for actinide systems [5–8] as well as to several review articles [9–13], a fairly complete bibliography [14] and two recent books [15,16] on relativistic electronic structure methods and their applications.

1.1. Relativistic and correlation effects in actinides

The actinides are among the most fascinating and challenging elements for a quantum chemist. Many aspects of their chemistry are discussed in this volume and only a few important aspects for first-principles electronic structure calculations will be mentioned here. Actinides and their ions frequently possess ground and/or many low-lying excited states with quite high values of total angular momentum, which are often composed from high spin and orbital angular momenta within an intermediate coupling scheme [17]. As an example the ground states of the neutral atoms and the up to fourfold charged cations are listed in Table 1. The valence shells 5f, 6d, 7s, 7p, etc., extend over three main quantum numbers and, although they are spatially quite well separated, they are energetically relatively close to each other [18], cf. Fig. 1 for the U $5f^3$ $6d^1$ $7s^2$ ground state configuration. In some cases this leads to several electronic configurations which are energetically quite close and may compete to contribute to chemical bonding.

Relativistic contributions increase with the fourth power of the nuclear charge and thus are very large for actinides. Since a large number of articles discussing relativistic effects in chemistry are available [9–13], only a very brief sketch of some important issues is given here. In one-electron atoms/ions all orbitals are stabilized and contracted by the so-called "direct relativistic effects" when the non-relativistic Hamiltonian is replaced by a relativistic one. Spin–orbit splitting lifts the degeneracy of the shells with $l > 0$ and leads to energetically lower and higher subshells with total angular momenta $j = l - 1/2$ and $j = l + 1/2$, respectively. In many-electron atoms the direct relativistic effects cause and are in competition with so-called "indirect relativistic effects", i.e. the contraction of mainly the inner s- and p-shells leads to a more efficient shielding of the nuclear charge for the outer shells of mainly d- and f-symmetry and thus tends to destabilize and expand these. As a result for the valence shells one usually finds stabilization and contraction of s- and p-shells (dominating direct relativistic effects) and destabilization and expansion of d- and f-shells (dominating indirect relativistic effects), cf. Fig. 1 for the U orbital energies. Clearly, these atomic effects on valence orbitals influence chemistry and lead, e.g. to bond length contractions/expansions and/or bond stabilizations/destabilizations [13].

Relativistic effects do not only lead to quantitative changes of the results of quantum chemical calculations, they sometimes even cannot be neglected for qualitative arguments. For example, at the non-relativistic Hartree–Fock (HF) level U would have a $5f^4$ $7s^2$ ground state configuration, with an energetically and spatially rather core-like 5f shell, ≈ 3.07 eV below the experimentally observed $5f^3$ $6d^1$ $7s^2$ ground state configuration and thus would be mainly divalent, whereas at the relativistic DHF level due to the stronger relativistic destabilization of the 5f shell

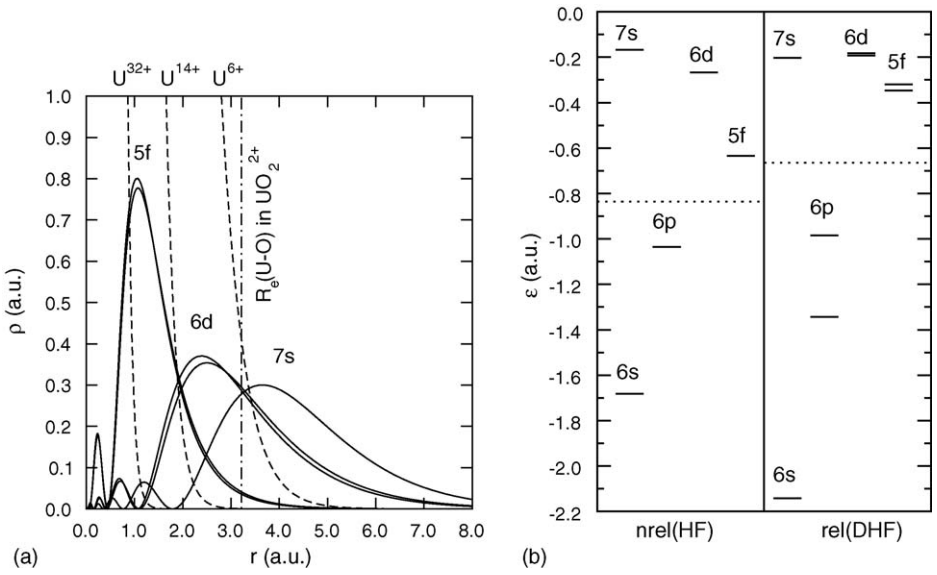

Fig. 1. (Left) Radial densities of the 5f, 6d and 7s valence spinors of U in the $5f^3\ 6d^1\ 7s^2$ ground state configuration in comparison to the radial densities of the U^{32+}, U^{14+} and U^{6+} cores from average-level multi-configuration Dirac–Hartree–Fock calculations [18]. (Right) Non-relativistic orbital energies (Hartree–Fock, HF) and relativistic spinor energies (Dirac–Hartree–Fock, DHF) for valence shells of U from average level calculations [18]. The horizontal dotted lines correspond to a "chemical" core-valence separation based on one-particle energies.

compared to the 6d shell $5f^4\ 7s^2$ is ≈ 2.04 eV above $5f^3\ 6d^1\ 7s^2$ [18]. Even larger differential relativistic effects have been found between the non-relativistic $5f^2\ 7s^2$ and the relativistic $6d^2\ 7s^2$ ground state configuration of Th [6]. Due to the lack of occupied 5f orbitals in its ground state Th is sometimes even looked at as a 6d transition element rather than a 5f element. We note however, that omitting the contributions of the Th 5f orbitals in compounds such as ThO leads to very poor results in quantitative studies [2].

Table 1 also reveals that for the higher ionization potentials of the actinides the 5f occupation number between start and end state often differs [17]. A similar observation is often made when the ground states of actinide compounds are compared to those of the neutral atoms, e.g. U is $5f^3\ 6d^1\ 7s^2$ in the ground state but $U^{IV}5f^2$ in uranocene $U(C_8H_8)_2$ (i.e. $U^{4+}(C_8H_8^{2-})_2$ in the limit of an ionic complex). The corresponding energy differences (excitation energies, ionization energies, binding energies, etc.) between states/systems with different 5f occupation number have large contributions from relativistic effects (stabilizing states/systems with a lower 5f occupation number) and electron correlation effects (stabilizing states/systems with a higher 5f occupation number) [19]. Electron correlation effects are usually large in spatial regions of high electron density, e.g. for the relatively compact 5f shells of the actinides since they are also embedded in other (closed) shells with a similar radial extent. Whereas today the relativistic contributions can be accounted for quite accurately by a number of computational schemes, among them effective core potentials (ECPs), the systematic inclusion of electron correlation effects is still a severe problem in many cases. Electron correlation effects tend to stabilize high occupation numbers in orbitals with high angular momentum, i.e. whereas relativistic effects prefer the occupation of orbitals in the order $s > p > d > f$, the opposite trend is found for electron correlation, i.e. $f > d > p > s$. A typical example for large relativistic and electron correlation contributions related to changes in the 5f occupation number, and thus the oxidation number, are the third and fourth ionization potential of the actinides, which are displayed in Fig. 2. The non-negligible spin–orbit effects contributing to the differential relativistic effects are separately shown in Fig. 3. Noting the magnitude of differential relativistic and electron correlation effects and keeping in mind that calcula-

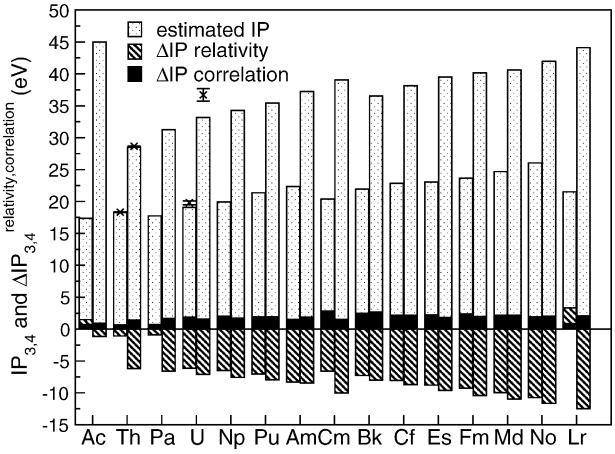

Fig. 2. Third (left bars) and fourth (right bars) ionization potentials of the actinides estimated by pseudopotential (PP) multi-reference averaged coupled-pair functional (MR-ACPF) calculations including spin–orbit corrections and extrapolation to the basis set limit (dotted bars) [19]. Relativistic contributions estimated from the difference of state-averaged multi-configuration Dirac–Hartree–Fock (Dirac–Coulomb–Breit Hamiltonian) and Hartree–Fock calculations (striped bars) [18] and electron correlation contribution estimated from PP MR-ACPF correlation energies extrapolated to the basis set limit (filled bars) [19]. Crosses with error bars denote the experimentally measured values for Th and the semiempirical estimates for U [17].

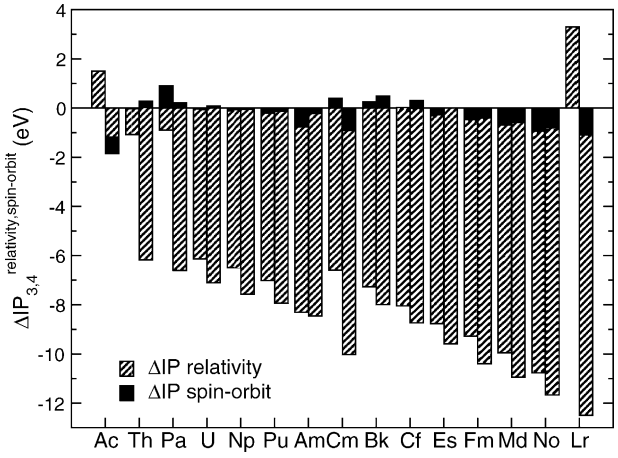

Fig. 3. Total relativistic contributions estimated from the difference of state-averaged Dirac–Hartree–Fock (Dirac–Coulomb–Breit Hamiltonian) and Hartree–Fock calculations (striped bars) [18] and spin–orbit contributions estimated from pseudopotential calculations with and without spin–orbit operator (filled bars) [19] to the third (left bars) and fourth (right bars) ionization potentials of the actinides.

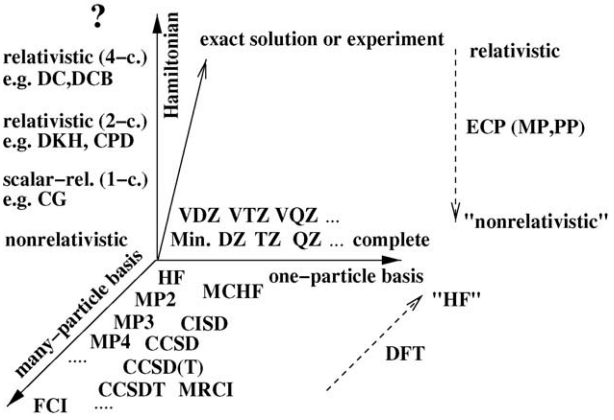

Fig. 4. Schematic representation of the effective core potential (ECP) approximation in a coordinate system of three axes determining the quality of the many-electron Hamiltonian, the one- and the many-electron basis sets.

tions of "chemical accuracy" have to be accurate to 0.05 eV, it is understandable that most of the first principles electronic structure calculations published so far avoid the calculation of energy differences between states/systems with different 5f occupation number.

1.2. Effective core potentials

Effective core potentials (ECPs) are almost as old as quantum mechanics [20,21]. The initial motivation for the method was to reduce the computational effort by replacing the chemically inert core shells of heavy atoms by effective potentials, i.e. only the chemically relevant valence electron system is treated explicitly in the presence of the ECP. This way, all elements of a group in the periodic table require essentially the same computational effort and thus can be treated with approximately the same accuracy. After the importance of relativistic contributions for the chemistry of heavy elements was fully realized about 25 years ago [9–11], relativistically parametrized ECPs offered a convenient way to include the major relativistic effects in formally non-relativistic calculations and soon became the method of choice for electronic structure calculations of heavy element compounds. Despite the improvements in the technology of fully relativistic (four-component) AE calculations and the development of quasi-relativistic (two- and one-component) transformed Hamiltonians such as the Douglas–Kroll–Hess (DKH) Hamiltonian [22], the modern ECP methods still seem to offer an attractive compromise between sufficiently high accuracy and low computational cost, especially for systems containing several heavy elements [23,24].

When judging the quality of quantum chemical ab initio calculations one has to keep a coordinate system with three axes in mind, i.e. a Hamiltonian axis and two axes for the one- and many-electron bases, cf. Fig. 4. Trying to approach the limit along one axis only is usually not a good idea, since the experimental values can only be approached by a reasonable compromise with respect to all three axes. Since the exact many-electron Hamiltonian is not known, one usually selects an approximation for it and then attempts to find in the plane of the one- and many-electron bases an as complete as possible but still computationally feasible combination. Hierarchies of optimized basis sets and computational methods are needed to systematically investigate the convergence of the calculated results towards the exact answer for the given Hamiltonian, which is hopefully close to the experimental values. The corresponding calculations are usually the more costly, the more accurate the many-electron Hamiltonian is, i.e. four-component AE schemes (spin and charge degrees of freedom, "fully relativistic") are computationally more costly than two-component AE schemes (spin degrees of freedom, "quasi-relativistic"), and the latter more costly than one-component AE schemes ("scalar-relativistic", non-relativistic). ECP approaches attempt to construct effective VO Hamiltonians for the valence electron system which are formulated at a lower level (quasi-relativistic or scalar-relativistic) and usually aim to reproduce the results of a higher computational AE method (e.g. fully relativistic). This way ECPs not only reduce the computational effort as compared to AE calculations, but they also allow to incorporate the most important relativistic effects into formally non-relativistic calculations. We note that the quality of the effective VO Hamiltonian can be checked by calibration calculations in two ways, i.e. by performing VO and AE calculations with nearly identical quality of the one- and many-electron bases or by extrapolating in the plane of the one- and many-electron bases to the basis set limit and comparing to experimental results.

At this point a comment is to be made on the usage of ECPs in DFT calculations. Most of the ECPs used today in molecular quantum chemistry are derived in the framework of ab initio calculations and can only be expected to work well for these. DFT attempts to map the many-electron problem to an effective one-electron problem (Kohn–Sham equations) and frequently functionals parametrized for AE systems composed of light elements are employed. Although in Fig. 4 DFT and ECP methods may appear to work along different axes (many-electron basis, respectively, Hamiltonian axis), due to the elimination of

the core electron system in ECPs they are not completely independent. Nevertheless, experience tells that so-called small-core ECPs may also be applied with good success in DFT calculations, although they are not derived for this purpose.

2. Energy-consistent pseudopotentials

2.1. Valence-only model Hamiltonian

The goal of ab initio ECP theory is to model relativistic AE calculations for a n electron system in the potential of N nuclei using an effective VO model Hamiltonian:

$$H_{\mathrm{v}} = \sum_{i}^{n_{\mathrm{v}}} h_{\mathrm{v}}(i) + \sum_{i<j}^{n_{\mathrm{v}}} g_{\mathrm{v}}(i,j) + V_{\mathrm{cc}} + V_{\mathrm{cpp}} \tag{1}$$

for

$$n_{\mathrm{v}} = n - \sum_{\lambda}^{N} (Z_\lambda - Q_\lambda) \tag{2}$$

explicitly treated valence electrons. Here and in the following the subscripts v and c refer to valence and core, respectively. i and j are electron indices, whereas λ and μ represent core indices. Q_λ stands for the charge of the core λ, whereas Z_λ is the actual nuclear charge. In the first two sums h_{v} and g_{v} stand for effective one- and two-electron VO operators, which are usually of a non-relativistic form, i.e.:

$$h_{\mathrm{v}}(i) = -\frac{1}{2}\Delta_i + V_{\mathrm{cv}}(i) \quad \text{and} \quad g_{\mathrm{v}}(i,j) = \frac{1}{r_{ij}} \tag{3}$$

The third term V_{cc} in Eq. (1) represents the repulsion between all cores and/or nuclei of the system, for which the leading contribution is the Coulomb repulsion between point charges represented by the first sum:

$$V_{\mathrm{cc}} = \sum_{\lambda<\mu}^{N} \left(\frac{Q_\lambda Q_\mu}{r_{\lambda\mu}} + \Delta V_{\mathrm{cc}}^{\lambda\mu}(r_{\lambda\mu}) \right) + \cdots \tag{4}$$

The correction term ΔV_{cc} arises for large cores with an extended electron density, i.e. it accounts for deviations from the point charge model when a neighboring nucleus penetrates a core density or when two core densities significantly overlap. The latter case also accounts for contributions of the Pauli repulsion between the electrons of the interacting cores. The fourth term V_{cpp} in Eq. (1) is a core polarization potential (CPP), accounting for static core polarization, i.e. deviations from the frozen-core approximation at the Hartree–Fock level, as well as dynamic core polarization, i.e. core-valence correlation effects.

The interaction of a valence electron with all nuclei and cores present in the system is described by the ECP V_{cv} in Eq. 3. The molecular ECP is assumed to be a superposition of atomic ECPs, with the Coulomb attraction between point charges as the leading term:

$$V_{\mathrm{cv}}(i) = \sum_{\lambda}^{N} \left(-\frac{Q_\lambda}{r_{\lambda i}} + \Delta V_{\mathrm{cv}}^{\lambda}(\vec{r}_{\lambda i}) \right) + \cdots \tag{5}$$

The correction term ΔV_{cv} has to incorporate all effects beyond the simple point charge model, e.g. interaction of a valence electron with an extended core density including the Pauli repulsion instead of a point charge, contributions arising from the orthogonality requirements between core and valence electron wavefunction and last but not least relativistic contributions. We note that the ECP should not only model these effects properly in an atom, but it should also be transferable without significant loss of accuracy to molecules, polymers or solids. In view of the various quite complicated interactions it can only be hoped that suitable parameterizations of simple ansaetze for $\Delta V_{\mathrm{cv}}^{\lambda}$, V_{cpp} and $\Delta V_{\mathrm{cc}}^{\lambda\mu}$ are able to compensate for all errors resulting from the simplifications of the original many-electron problem.

ECPs come in two varieties, model potentials (MPs) and pseudopotentials (PPs). MPs, e.g. the ab initio MPs of Seijo et al. [25], can be viewed to be a direct modelling of frozen-core AE calculations, e.g. the Fock operator for a valence electron system is simplified by removal of the core electrons and introduction of one-electron potentials and projection operators acting on the valence electrons without changing the nodal structure of the valence orbitals. PPs rely, in contrast to MPs, on the so-called pseudo-valence orbital transformation, i.e. in case of an atom the valence orbital or better pseudo-valence orbital lowest in energy for each angular quantum number l or lj is nodeless. Whereas most of the PPs are of the so-called shape-consistent type and use one-particle properties like orbitals/spinors and their energies as reference data, e.g. the PPs of Ermler and coworkers [26,27] or Hay and Martin [28], the energy-consistent PPs discussed here rely only on quantum mechanical observables like total valence energies [2].

For modern quasi-relativistic PPs, i.e. including spin–orbit coupling, a semilocal ansatz in two-component form was found to be a reasonable compromise between accuracy and efficiency:

$$\Delta V_{\mathrm{cv}}^{\lambda}(\vec{r}_{\lambda i}) = \sum_{l=0}^{L-1} \sum_{j=|l-1/2|}^{l+1/2} (V_{lj}^{\lambda}(r_{\lambda i}) - V_L^{\lambda}(r_{\lambda i})) P_{lj}^{\lambda}(i) + V_L^{\lambda}(r_{\lambda i}) \tag{6}$$

P_{lj}^{λ} projects onto spinor spherical harmonics centered at the core λ:

$$P_{lj}^{\lambda}(i) = P_{l,l\pm1/2}^{\lambda}(i) = P_{\kappa}^{\lambda}(i) = \sum_{m_j=-j}^{j} |\, \lambda l j m_j(i) \rangle \langle \lambda l j m_j(i) \,| \tag{7}$$

If spin–orbit coupling is neglected, i.e. for scalar quasi-relativistic calculations, a one-component form may be derived by averaging over spin:

$$\Delta V_{\mathrm{cv,av}}^{\lambda}(\vec{r}_{\lambda i}) = \sum_{l=0}^{L-1} (V_l^{\lambda}(r_{\lambda i}) - V_L^{\lambda}(r_{\lambda i})) P_l^{\lambda}(i) + V_L^{\lambda}(r_{\lambda i}) \tag{8}$$

Now P_l^{λ} projects onto the spherical harmonics centered at the core λ:

$$P_l^{\lambda}(i) = \sum_{m_l=-l}^{l} |\, \lambda l m_l(i) \rangle \langle \lambda l m_l(i) \,| \tag{9}$$

Table 2
Relative Dirac–Hartree–Fock/Dirac–Coulomb (DHF/DC) energies (eV) of the $2J+1$-weighted average of all J levels belonging to a non-relativistic configuration [18] with respect to the value for the U [Rn] $5f^3\ 6d^1\ 7s^2$ ground state configuration. Only subconfigurations outside the Rn core are listed (conf)

Charge	Configuration			AE		Frozen-core error		
	5f	6d	7s	DHF/DC	+B	$Q=32$	$Q=14$	$Q=6$
6+				167.9498	0.3263	0.0077	1.2479	15.4283
5+		1		118.1617	0.3208	0.0058	1.0291	11.3885
4+		2		78.6962	0.3138	0.0048	0.8850	8.2895
3+		3		49.0026	0.3061	0.0043	0.7963	6.0066
2+		4		28.4542	0.2984	0.0040	0.7488	4.4237
1+		4	1	16.0181	0.3111	0.0039	0.7379	3.8610
0		4	2	9.7540	0.3200	0.0038	0.7365	3.5686
5+	1			107.4044	0.1997	0.0021	0.4545	7.1973
4+	1	1		69.4125	0.1942	0.0014	0.3779	4.8002
3+	1	2		41.0364	0.1878	0.0014	0.3359	3.1180
2+	1	3		21.6260	0.1812	0.0013	0.3179	2.0282
1+	1	3	1	9.6394	0.1929	0.0013	0.3082	1.6778
0	1	3	2	3.6701	0.2007	0.0013	0.3046	1.5126
4+	2			62.9423	0.0850	0.0003	0.0886	2.3845
3+	2	1		35.8785	0.0804	0.0002	0.0765	1.2558
2+	2	1	1	17.5395	0.0938	0.0002	0.0682	0.8277
1+	2	1	2	5.7548	0.1031	0.0001	0.0636	0.5841
0	2	2	2	0.4682	0.0933	0.0002	0.0678	0.3493
3+	3			33.3768	−0.0147	0.0000	0.0006	0.3479
2+	3		1	15.7154	−0.0015	0.0000	0.0006	0.1366
1+	3		2	4.4832	0.0073	0.0000	0.0009	0.0412
0	3	1	2	0.0000	0.0000	0.0000	0.0000	0.0000
2+	4			17.2536	−0.0932	0.0002	0.0467	0.2082
1+	4		1	6.8681	−0.0817	0.0001	0.0450	0.2224
0	4		2	2.0435	−0.0749	0.0002	0.0426	0.2430
1+	5			12.5023	−0.1358	0.0004	0.0945	0.6651
0	5		1	8.1022	−0.1171	0.0004	0.0761	0.5418

For each f occupation number only the energetically lowest configuration for each ionization level is listed. Contributions of the Breit interaction evaluated in first-order perturbation theory are also given (+B). The frozen-core errors (eV) in the relative energies are given for 32, 14 and 6 valence electron systems. The frozen core was taken from the neutral atom in the ground state configuration. Frozen cores: U $Q=6$: 1s–5d, 6s, 6p; $Q=14$: 1s–5d; $Q=32$: 1s–4d.

A corresponding spin–orbit operator can be defined as

$$\Delta V^{\lambda}_{\mathrm{cv,so}}(\vec{r}_{\lambda i}) = \sum_{l=1}^{L-1} \frac{\Delta V^{\lambda}_{l}(r_{\lambda i})}{2l+1} [l P^{\lambda}_{l,l+1/2}(i) - (l+1) P^{\lambda}_{l,l-1/2}(i)] \tag{10}$$

with the difference between the two-component PPs:

$$\Delta V^{\lambda}_{l}(r_{\lambda i}) = V^{\lambda}_{l,l+1/2}(r_{\lambda i}) - V^{\lambda}_{l,l-1/2}(r_{\lambda i}) \tag{11}$$

The potentials V^{λ}_{lj}, V^{λ}_{l}, V^{λ}_{L} and ΔV^{λ}_{l} are usually represented as linear combinations of Gaussians multiplied by powers of the electron-core distance. In case of the energy-consistent PPs discussed here the local term V^{λ}_{L} is omitted. The exact partitioning of a many-electron system into subsystems such as core and valence is not possible in quantum mechanics, since the electrons are elementary particles and therefore indistinguishable. An approximate core-valence separation can only be achieved within the framework of effective one-particle theories like HF or DHF. However, even the VO model Hamiltonians resulting from a strict derivation in this limited framework are by far too complicated to be of use in practical calculations. Therefore, usually a VO model Hamiltonian is formulated with free parameters (coeffcients and exponents of Gaussians expansions of the radial potentials) which are adjusted to reproduce reference data derived from more rigorous AE calculations.

2.2. Choice of the core

One of the most important choices for the construction of EPCs is, besides the selection of reliable reference data, the choice of the core. Here a compromise between the desired high accuracy and low computational cost is seeked. A very good indication if an ECP will yield accurate results can be obtained from atomic AE frozen-core calculations. The non-local HF or DHF operator acting on the valence shell of an atom is essentially the best VO operator one can construct. Since U is probably the most important element of the actinide series, we took it as an example and performed for various electronic configurations of U and its cations up to U^{6+} state-averaged multi-configuration DHF AE calculations using the DC Hamiltonian and estimating the Breit-contributions in first-order perturbation theory [18]. The results are listed in Table 2. The entries are ordered according to increasing 5f occupation number and for a given 5f occupation number according to increasing 6d occupation number. The energies are given relative to the U $5f^3\ 6d^1\ 7s^2$ ground state configuration. The relatively small contributions of the Breit term given in the second column usually amount to 5% or less

of the total energy difference listed in the first column. An exception is the low-energy excitation $5f^3\ 6d^1\ 7s^2 \rightarrow 5f^2\ 6d^2\ 7s^2$, where the Breit term contributes with 16%. It is noteworthy that the contributions are quite similar for all configurations with a given 5f occupation number and appear to increase smoothly from ≈ -0.1 eV for $5f^5$ to $\approx +0.3$ eV for $5f^0$.

The frozen core errors for three different sizes of the frozen core are listed in the last three columns. $Q = 32$ refers to a 32 valence electrons, i.e. 60 core electrons in $1s^2 \ldots 4f^{14}$. The frozen core errors are less than ≈0.01 eV for all cases considered here and thus ECPs adopting such a small-core definition should exhibit only small errors. $Q = 14$ denotes a core in which in addition the $5s^2\ 5p^6\ 5d^{10}$ semi-core shells are included, i.e. 14 valence electrons are treated explicitly. One observes a clear dependency of the errors on the 5f occupation number, whereas only smaller variations of the errors occur with changing 6d occupation number for a given 5f occupation number. In our opinion the corresponding medium-core ECPs may be useful for many purposes, however, energy differences between states/systems differing in their 5f occupation number have to be interpreted with great care. Corresponding medium-core PPs have been derived (but not published) [29], but usually yield less accurate results than the small-core PPs. Finally, the choice of the core based on chemical intuition, i.e. $Q = 6$ referring to six valence electrons and a $1s^2 \ldots 5d^{10}\ 6s^2\ 6p^6$ core, leads to much too large errors in order to be meaningful.

The reason for the behavior of the frozen-core errors summarized in Table 2 is obvious from Fig. 1. Energetically, i.e. judged from their orbital energies, the 5f, 6d and 7s valence orbitals are well separated from the 6s and 6p semi-core shells as well as the energetically even lower other core shells. However, geometrically, e.g. based on their radial densities the 6s and 6p shells are more diffuse than the 5f shell. Since the radial density of the 5f shell is more compact than the total radial density of U^{6+} (large-core) or U^{14+} (medium-core), a change in the 5f occupation number by one changes the effective nuclear charge for the outer orbitals by ≈1 and the frozen-core approximation is doomed. Considering the 6d shell it is obvious, that a change in the 6d occupation number will have only a moderate effect on the more compact U^{14+} core density, but again leads to a breakdown of the frozen-core approximation for the more diffuse U^{6+} core.

2.3. Pseudopotential parameter adjustment

The parameters of the energy-consistent actinide PPs were adjusted to total valence energies derived from finite-difference AE scalar-relativistic HF calculations performed within the so-called Wood–Boring scheme [2]. For a multitude of low-lying electronic states of the neutral atom and its low-charged ions pseudopotential finite difference calculations are required to yield in a least-squares sense total valence energies E_I^{PP} as close as possible to corresponding AE values E_I^{AE}, i.e.:

$$\sum_I (w_I [E_I^{PP} - E_I^{AE}]^2) := \min \tag{12}$$

Valence spin–orbit operators have recently been readjusted based on fine-structure splittings derived at the AE MCDHF level using the Dirac–Coulomb (DC) Hamiltonian and estimating the Breit (B) contributions in perturbation theory [3]. Two parametrizations are offered, one for use in perturbation theory using scalar-relativistic orbitals and one in either variational calculations and/or spin–orbit CI calculations accounting for orbital relaxation under the spin–orbit operator. It should be noted that both sets assume 5s, 5p, 5d semi-core shells frozen in their scalar-relativistic form. Within the appropriate scheme the accuracy of both spin–orbit operators is similar, however, care has to be taken since application in the wrong scheme might lead either to double counting or to neglect of orbital relaxation under the spin–orbit operator. The restriction of the space on which the spin–orbit operators may act (5f, 6d, (7s), 7p and higher orbitals in each symmetry) is both a strength and a weakness. On one hand the approach is very efficient and allows to take spin–orbit effects into account at very low computational cost. On the other hand the PPs are not suitable for application in two-component variational calculations or SO-CI calculations with excitations from the inner shells and thus results cannot be compared to AE MCDHF data, a drawback especially for molecular calibration studies. Therefore, future PP adjustments for actinides also should be directly based on AE MCDHF/DCB reference data, similar to recent work on main group atoms and d-transition metals [30–32].

2.4. Optimization of valence basis sets

Valence basis sets using a segmented [3] as well as a generalized [4] contraction scheme have recently been optimized for the actinide small-core energy-consistent PPs. These sets are analogous to the ones available for the corresponding lanthanide small-core PPs [33–35]. The (14s13p10d8f6g)/[6s6p5d4f3g] atomic natural orbital valence basis sets have been optimized to describe as well as possible the most important configurations with different 5f occupancy, e.g. $5f^{n+1}\ 7s^2$ and $5f^n\ 6d^1\ 7s^2$. They are roughly of polarized valence quadruple-zeta quality, however, since a generalized contraction scheme was strictly applied, smaller sets of polarized triple-zeta or double-zeta quality can be obtained with the same set of primitives by just omitting the contractions with the lowest natural occupation number, e.g. (14s13p10d8f6g)/[5s5p4d3f2g] or (14s13p10d8f6g)/[4s4p3d2f1g]. The (14s13p10d8f6g)/[10s9p5d4f3g] sets using a segmented contraction have been derived from the above generalized contracted ANO sets and also yield results of quadruple-zeta quality.

3. Calibration calculations

3.1. Atomic ionization potentials and excitation energies

Test calculations for the first to fourth atomic ionization potentials as well as 5f–6d and 6d–5f excitation energies have been published [3,19,36]. Spin–orbit corrected PP MR-ACPF results were compared to fully relativistic AE Dirac–Kohn–Sham (DKS) results using gradient-corrected density functionals [36] and, as far as it is available, to experimental data [17]. The PP calculations have been repeated later with the new generalized

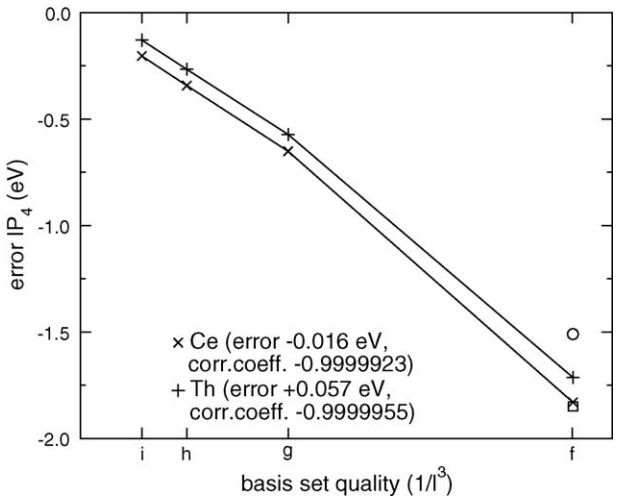

Fig. 5. Errors in spin–orbit corrected coupled-cluster singles, double and perturbative triples results for IP_4 of Ce and Th. The experimental values are 36.76 and 28.65 eV for Ce and Th, respectively. The errors of uncorrelated calculations are denoted by a circle and square for Ce and Th, respectively. Relativistic energy-consistent small-core ab initio pseudopotentials (32 valence electrons) and large uncontracted basis sets (16s15p12d10f8g8h8i for Ce and 14s13p10d8f6g6h6i for Th) have been applied. The errors for basis sets including functions up to angular quantum number l are linear in $1/l^3$ for $l > 3$ and can be extrapolated to the basis set limit.

and segmented contracted basis sets [3,4] as well as with very large uncontracted basis sets and basis set extrapolation techniques partly using the CCSD(T) approach [19]. Since almost all higher IPs of actinides are yet experimentally not determined and no systematic investigations at the AE ab initio level exist, these values may serve as estimates. Fig. 5 demonstrates such basis set extrapolation studies for the fourth ionization potentials of Ce and Th. Although the PPs have not been adjusted to such highly ionized states, they appear to reproduce the higher IPs in case of the lanthanides quite well with errors of at most a few tenths of an electronvolt and a similar performance is expected for the actinides [37].

3.2. Diatomic molecules

The transferability of ECPs from the atom to a molecular or solid state environment should always be checked carefully, especially for large-core approximations. The small-core energy-consistent PPs for actinides have been successfully tested for a number of diatomics, e.g. AnX (An = Ac, Lr; X = H, O, F) and ThO [2,3], both by comparison to AE as well as to experimental data. As an example recent results or the $^1\Sigma^+$ ground state of ThO using the newly optimized valence basis sets are listed in Table 3 [3]. A very small basis set superposition error is observed, both at the uncorrelated and the correlated level. At the CCSD(T) level the bond length and vibrational frequency are in excellent agreement with experimental data. After correcting for the atomic and molecular spin–orbit lowerings as well as for the zero-point energy the counter-poise corrected value for the dissociation energy of 8.96 eV agrees very well with the various experimental values ranging from 8.79 ± 0.13 to 9.00 ± 0.09 eV.

Table 3
Bond lengths R_e (Å), vibrational constants ω_e (cm^{-1}) and binding energies D_e (eV) of ThO in the $^1\Sigma^+$ ground state from energy-consistent small-core pseudopotential calculations [3] in comparison to experimental data

Method	R_e	ω_e	D_e	D_0[a]
SCF[b]	1.817/1.817	956/955	6.26/6.24	
SCF/CCSD(T)[b]	1.839/1.845	898/891	9.58/9.38	9.16/8.96
Exp.	1.840	896		9.00±0.09
				8.87 ± 0.15
				8.79 ± 0.13

The calculated values are given without/with Boys–Bernardi counter-poise correction of the basis set superposition error.

[a] Theoretical D_e values have been corrected for molecular (0.03 eV) and atomic (Th 0.38, O 0.01 eV) spin–orbit energy lowerings; the zero-point energy (0.06 eV) was subtracted to obtain D_0 [2].

[b] PP with 60 core-electrons [2], basis sets Th (14s13p10d8f6g)/[6s6p5d4f3g] ANO [3], O aug-cc-pVQZ (spdfg); Th 5s,5p and O 1s frozen in CCSD(T).

4. Selected applications

A selection applications of energy-consistent relativistic small-core PPs to polyatomic molecules [38–69] mainly carried out by other groups during the last 5 years is presented in Table 4. The by far majority of these studies applied the PPs in combination with DFT, which appears to give quite satisfactory results. However, the question which functionals perform best, does not seem to be finally settled, i.e. whereas some authors recommend the generalized gradient approximation (GGA) [43,49,50], others find hybrid functionals to perform better [63,64]. In many of these studies also large-core PPs both of the energy-consistent and the shape-consistent type have been applied and their deficiencies became especially obvious in DFT calculations, e.g. ≈0.02–0.03 Å too short bond lengths in UO_2^{2+} and UF_6 [49,63], but ≈ 0.04 Å too long bond lengths in UCl_3 [51]. As an example for the reliability of the small-core PPs we mention here UF_6 from the work of Batista et al. [63], since this study already applies the newly optimized valence basis sets [3] as well as the work of Han and Hirao [49] still applying the older basis sets. Table 5 reveals that both U–F bond length as well as the infrared frequencies and intensities of the various PP DFT calculations agree well with experimental data. For the U–F bond dissociation energy the hybrid functionals PBE0 and B3LYP give the best results.

5. Outlook

Shortcommings of the presently used set of energy-consistent small-core PPs for the actinides are mainly to be seen in the use of quasi-relativistic AE reference data, i.e. Wood–Boring HF data instead of MCDHF data based on the DC Hamiltonian and a perturbative estimate of the Breit contributions. However, the adjustment of such PPs is a tremendous computational task, mainly due to the large number of LSJ levels (up to $O(10^4)$) arising for each (non-relativistic) configuration with open 5f, 6d, etc., shells, which have to be calculated in every iteration (up to $O(10^3)$) of the fitting process. The technology for such adjustments is at hand and they already have been performed successfully for heavy main group as well as transition metals

Table 4
Overview over recent calibration studies and applications of energy-consistent relativistic small-core actinide pseudopotentials in chronological order

Systems[a]	Methods[b]	Properties[c]	Ref.
$Th(C_8H_8)_2$	MP2, MRCI, ACPF, SO-CI	S,V,E	[38]
$U(C_8H_8)_2$	MRCI, ACPF, SO-CI	S,V,E	[39]
$An(C_6H_6)_2$ (An = Th, U)	MP2, CCSD(T)	S,B	[40]
$Th(C_6H_6)_2$	BP86	S,B	[41]
NUO^+, NUO, NThO	BP86, B3LYP	S,V,I	[42]
AnO_2^{2+} (An = U,Pu)	SVWN, BP86, B3LYP, HF, MP2, MP4, MRCI, MCPF, AQCC, CCSD	S,V,E	[43]
PuO_2^{2+}	CASPT2, AQCC, MRCI	S,E	[44]
$UO_2^{2+}H_n$ (n = 0, 1, 2)	HF, CASPT2, ACPF, B3LYP, SO	S,B	[45]
$AnO_2^{2+}H_n$(n = 0, 1, 2)	RASSCF, AQCC, SO	S,B	[46]
ThX_4 (X = F, Cl, Br, I)	SVWN, B(3)LYP, HF, MP2	S,V	[47]
XUY (X,Y = C, N, O)	B3LYP, CASPT2	S,V	[48]
UO_2^{2+}, AnF_6 (An = U, Np, Pu)	SVWN, B(3)LYP/PW91, PWPW91, CCSD(T)	S,V	[49]
AnF_6 (An = U, Np, Pu), $UF_{6-n}Cl_n$ (n = 1–6)	B3LYP/P86/PW91, B1LYP, mPW1LYP/PW91	S,V	[50]
UCl_3	B(3)P86, B3LYP, PBE0, MP2	S,V	[51] [52]
AcO_2^{2+}, AnF_6 (An = U, Np)	SVWN, BP	S,V	[53]
CUO	CASPT2	S,V,E	[54]
I_3U–$NCCH_3$	PBE(0)	S	[55]
UO_2^{2+} $(C_2O_4)_2^{2-}$	HF, MP2	S,B	[56]
$CUO(Ne)_x(Ng)_n$	PW91	S,V,E	[57]
$(An(H_2O)_9)^{3+}$,$(AnZ(H_2O)_6)^{3+}$, $(AnZ(H_2O)_6Cl)^{2+}$, (An = U, Pu, Am, Cm)	BP86, B3LYP, MP2	S	[58]
AmF_3, $AmCl_3$	CASSCF, CASPT2	S,E	[59]
UO_2^{2+}, NUN, NUO^+, CUO	SVWN, B(3)LYP/PW91, B97, PBE(0)	S,V	[60]
PuO_2^{2+}, PuN_2	SVWN, B(3)LYP/PW91, CASPT2,DDCI	S,V,E	[61]
CUO(Ng) (n = 1–4)	PW91	S,V,E	[62]
UF_6, UF_5	HF, PBE(0), B3LYP	S,V,B	[63]
UF_n, UCl_n	B3LYP, PBE0	S,V,B	[64]
UO_2^{2+}–UO_2^+ complexes	CASPT2	S,T	[65]
NpO_2^{2+}–NpO_2^+ complexes	CASPT2	S,T	[66]
NpO_2^{2+}–NpO_2^+ complexes	SO-CI	S,T	[67]
$UF_{6-n}Cl_n$ (n = 1–6)	B(3,H)LYP/P86, B(3,H)PW91	S,N	[68]
AnX_6 (An = Th–Np;X = H, F)	B3LYP	S	[69]

[a] Z = 2,2′:6′ 2″-terpyridine, 2,6-bis(5,6-dimethyl-1,2,4-triazin-3-yl)pyridine; Ng = Ar, Kr, Xe.

[b] For an explanation of the (standard) acronyms characterizing the computational method the reader is referred to the original articles; short hand notations: B3LYP/PW91 = B3LYP, B3PW91; B(3)LYP/PW91 = BLYP, B3LYP, BPW91, B3PW91; PBE(0) = PBE, PBE0; etc.

[c] S: structure optimisation; B: binding (and/or reaction) energy; V: vibrational frequencies; I: infrared intensities; E: electronic excitation energies; N: nuclear magnetic resonance data; T: electron transfer rate constants.

for up to several thousand LSJ levels [30–32]. One advantage would be the implicit account of relativistic effects including the Breit interaction, which is quite costly to include fully at the AE level. Other computationally very attractive options leading to significant savings compared AE work also at the correlated level are large-core CPPs and/or SO operators in connection with small-core PPs [34].

Since partially occupied 5f shells generate often large problems in ab initio calculations and, in some cases, a detailed knowledge of structure and contributions of the 5f shell is not required, the construction of 5f-in-core pseudopotentials modelling actinide ions/atoms with a fixed valency/5f-occupation appears to be a promising route towards more approximate studies for the future. Table 2 shows relatively constant errors in the column Q = 14 for a given 5f occupation and implies that, in analogy to the frequently applied 4f-in-core PPs of the lanthanides (cf. [8] and references cited therein), also 5f-in-core PPs for the actinides could be constructed. Since the 5f shell becomes more core-like along the actinide series, it is expected that the approach works better for the heavier than for the lighter actinides. In fact, corresponding PPs for trivalent actinides with 11 valence electrons and a $1s^2 \ldots 5f^n$ core (n = 0–14 for Ac–Lr) have been derived [70] and despite the rough underlying approximation appear to work surprisingly well in those cases where the 5f shell does not contribute to bonding too much. An example are complexes of An^{3+} with water, where 5f-in-core PP HF results [70] compare very well to AE DHF data [71] as well as to results obtained with small-core PPs [2,3], cf. Table 6. We note that the atomic actinide AE total DHF energies obtained with finite basis sets differ by 0.4–1.7 eV from the finite difference

Table 5
Comparison of the U–F bond length R_e (Å), the infrared frequencies ν_i (cm^{-1}) and the bond dissociation energy D_e (kcal/mol) of UF_6 from various pseudopotential density functional theory calculations to experimental data

Method	R_e	ν_1, a_{1g}	ν_2, e_g	ν_3, t_{1u}	ν_4, t_{1u}	ν_5, t_{2g}	ν_6, t_{2u}	D_e	Ref.
HF	1.980	740	541	655	199	221	143		[49]
	1.985	741	546	659 (1064)	201 (83)	222	143	−3.2	[63]
SVWN	1.989	661	546	627	171	183	130		[49]
	1.993	660	548	628 (594)	173 (30)	184	130	117.7	[63]
BLYP	2.035	611	509	579	176	187	130		[49]
BPW91	2.019	624	517	591	176	187	131		[49]
PBE	2.021	625	519	593 (562)	176 (32)	186	131	95.6	[63]
B3LYP	2.007	657	530	613	184	196	138		[49]
	2.011	656	532	613 (685)	186 (41)	198	139	72.1	[63]
B3PW91	1.996	666	535	622	184	195	139		[49]
PBE0	1.993	677	532	631 (735)	186 (40)	198	140	70.7	[63]
CCSD(T)	2.002								[49]
Exp.	1.999	667	534	626 (750)	186 (38)	200	143	70 ± 2	
	1.996							69 ± 5	
								73	

The intensities of the main peaks are listed in parentheses. For explanation of the (standard) acronyms characterizing the computational method as well as references for experimental values see Refs. [49,63].

Table 6
Bond length (Å) and binding energies (eV) of actinide(III) monohydrate complexes $An(H_2O)^{3+}$ from 5f-in-core (LC) and 5f-in-valence (SC) pseudopotential (PP) Hartree–Fock [70] and all-electron (AE) Dirac–Hartree–Fock [71] calculations

An	R_e			D_e			n5f
	PP LC	PP SC	AE	PP LC	PP SC	AE	PP SC
Ac	2.47/2.45	2.47/2.45	2.45	3.55/3.25	3.55/3.33	3.62	0.03
Am	2.33/2.32	2.31/2.29	2.29	4.08/3.79	4.18/3.97	4.30	6.02
Cm	2.31/2.30	2.30/2.28	2.27	4.16/3.87	4.22/4.01	4.37	7.02
Es	2.26/2.25	2.24/2.23	2.23	4.39/4.10	4.46/4.27	4.59	10.02
Lr	2.19/2.19	2.20/2.19	2.21	4.69/4.40	4.70/4.51	4.85	14.01

The PP results are given for small/large basis sets. The 5f Mulliken population is also listed. Basis sets: AE An (30s25p19d13f2g), O (9s4p1d), H (4s1p) for large components; PP small basis sets: LC An (8s7p6d2f); PP SC An (14s13p10d8f)/[6s6p5d4f], O and H cc-pVDZ; PP large basis sets: LC An (8s7p6d2f1g); PP SC An (14s13p10d8f6g)/[6s6p5d4f3g], O and H aug-cc-pVQZ.

values, whereas in the PP case the corresponding deviations are less than 0.2 and 0.08 eV for the small-core (5f-in-valence) and large-core (5f-in-core) PPs, respectively. Therefore, it is likely that the AE values listed in Table 6 are affected by larger basis set superposition errors than the PP results.

Thus, a number of options exist to generate more accurate as well as computationally less demanding sets of PPs for actinides.

6. Conclusions

The development of relativistic energy-consistent ab initio pseudopotentials as well as corresponding optimized valence basis sets has been described and results of selected calibration calculations and applied studies have been discussed. Small-core actinide pseudopotentials reproduce very well the results of more rigorous all-electron studies based on relativistic Hamiltonians, but at a lower computational cost. It was emphasized that pseudopotentials, especially when spin–orbit interaction is taken into account, offer additional possibilities of computational savings without too big losses in accuracy, e.g. by means of the definition of effective spin–orbit operators for use in first-order perturbation theory for the (chemical) valence shells. The reliability of a recent very approximate 5f-in-core pseudopotential approach was established for monohydrate complexes of actinide(III) ions, but has to be further investigated in future especially for the lighter actinide elements.

Acknowledgements

X. Cao acknowledges the support of the German Academic Exchange Service (DAAD, D/03/314349) and the hospitality of the Theoretical Chemistry Group at Beijing Normal University (Prof. Dr. Wei-Hai Fang) during her visit, where part of this manuscript has been prepared.

References

[1] P. Pyykkö, Inorg. Chim. Acta 139 (1987) 243.
[2] W. Küchle, M. Dolg, H. Stoll, H. Preuss, J. Chem. Phys. 100 (1994) 7535.
[3] X. Cao, M. Dolg, H. Stoll, J. Chem. Phys. 118 (2003) 487.
[4] X. Cao, M. Dolg, J. Mol. Struct. (Theochem) 673 (2004) 203.
[5] M. Pepper, B. Bursten, Chem. Rev. 91 (1991) 719.
[6] M. Dolg, in: P.V.R. Schleyer, N.L. Allinger, T. Clark, J. Gasteiger, P.A. Kollman, H.F. Schaefer III, P.R. Schreiner (Eds.), The Encyclopedia of Computational Chemistry, Wiley, Chichester, 1998, p. 1478.

[7] G. Schreckenbach, P.J. Hay, R.L. Martin, J. Comput. Chem. 20 (1999) 70.
[8] M. Dolg, X. Cao, in: K. Hirao, Y. Ishikawa (Eds.), Recent advances in computational chemistry, vol. 6, World Scientific, New Jersey, 2004, p. 1.
[9] P. Pyykkö, Adv. Quant. Chem. 11 (1978) 353.
[10] K.S. Pitzer, Acc. Chem. Res. 12 (1979) 271.
[11] P. Pyykkö, J.-P. Desclaux, Acc. Chem. Res. 12 (1979) 276.
[12] P. Pyykkö, Chem. Rev. 88 (1988) 563.
[13] W.H.E. Schwarz, in: Z.B. Maksić (Eds.), Theoretical Models of Chemical Bonding, vol. 2: The Concept of the Chemical Bond, Springer, Berlin, 1990, p. 593.
[14] P. Pyykkö, Relativistic Theory of Atoms and Molecules 1915 – (RTAM) database, Version 11.0, 2005. http://www.csc.fi/rtam.
[15] B.A. Heß (Ed.), Relativistic Effects in Heavy-Element Chemistry and Physics, Wiley, Chichester, 2002.
[16] P. Schwerdtfeger (Ed.), Relativistic electronic structure theory. Part 1. Fundamentals, Elsevier, Amsterdam, 2002;
P. Schwerdtfeger (Ed.), Relativistic electronic structure theory. Part 2. Applications, Elsevier, Amsterdam, 2004.
[17] J. Blaise, J.-F. Wyart, Energy levels and atomic spectra of actinides, International Tables of Selected Constants, vol. 20, CNRS, Paris, 1992.
[18] K.G. Dyall, I.P. Grant, C.T. Johnson, F.A. Parpia, E.P. Plummer, Comput. Phys. Commun. 55 (1989) 425 (atomic structure code GRASP).
[19] X. Cao, M. Dolg, Mol. Phys. 101 (2003) 961.
[20] H. Hellmann, J. Chem. Phys. 3 (1935) 61.
[21] P. Gombás, Z. Phys. 94 (1935) 473.
[22] B.A. Hess, M. Dolg, B.A. Hess (Eds.), Relativistic Effects in Heavy-Element Chemistry and Physics, Wiley Series in Theoretical Chemistry, vol. 12, Wiley, New York, 2002, p. 89.
[23] M. Dolg, J. Grotendorst (Eds.), Modern Methods and Algorithms of Quantum Chemistry, NIC Series, Vol. 1, John Neumann Institute for Computing, Jülich, 2000, p. 479 ;
M. Dolg, J. Grotendorst (Eds.), Modern Methods and Algorithms of Quantum Chemistry, NIC Series, Vol. 3, John Neumann Institute for Computing, Jülich, 2000, p. 507.
[24] M. Dolg, P. Schwerdtfeger (Eds.), Relativistic Electronic Structure Theory. Part 1. Fundamentals, Elsevier, Amsterdam, 2002, p. 793.
[25] L. Seijo, Z. Barandiaran, E. Harguindey, J. Chem. Phys. 114 (2001) 118.
[26] W.C. Ermler, R.B. Ross, P.A. Christiansen, Int. J. Quant. Chem. 40 (1991) 829.
[27] C.S. Nash, B.E. Bursten, W.C. Ermler, J. Chem. Phys. 106 (1997) 5133.
[28] P.J. Hay, R.L. Martin, J. Chem. Phys. 109 (1998) 3875.
[29] Clickable periodic table with energy-consistent PPs and corresponding valence basis sets. http://www.theochem.uni-stuttgart.de.
[30] M. Dolg, H. Stoll, H. Preuß, R.M. Pitzer, J. Phys. Chem. 97 (1993) 5852.
[31] H. Stoll, B. Metz, M. Dolg, J. Comput. Chem. 23 (2002) 767.
[32] M. Dolg, Theor. Chem. Acc. 114 (2005) 297.
[33] M. Dolg, H. Stoll, H. Preuß, J. Chem. Phys. 90 (1989) 1730.
[34] X. Cao, M. Dolg, J. Chem. Phys. 115 (2001) 7348.
[35] X. Cao, M. Dolg, J. Mol. Struct. (Theochem) 581 (2002) 139.
[36] W. Liu, W. Küchle, M. Dolg, Phys. Rev. A 58 (1998) 1103.
[37] X. Cao, M. Dolg, Chem. Phys. Lett. 349 (2001) 489.
[38] M. Dolg, P. Fulde, H. Stoll, H. Preuß, R.M. Pitzer, A. Chang, Chem. Phys. 195 (1995) 71.
[39] W. Liu, M. Dolg, P. Fulde, J. Chem. Phys. 107 (1997) 3584.
[40] G. Hong, F. Schautz, M. Dolg, J. Am. Chem. Soc. 121 (1999) 1502.
[41] M. Dolg, J. Chem. Inf. Comp. Sci. 41 (2001) 18.
[42] M. Zhou, L. Andrews, J. Chem. Phys. 111 (1999) 11044.
[43] N. Ismail, J.-L. Heully, T. Saue, J.-P. Daudey, C.J. Marsden, Chem. Phys. Lett. 300 (1999) 296.
[44] L. Maron, T. Leininger, B. Schimmelpfennig, V. Vallet, J.-L. Heully, C. Teichteil, O. Gropen, U. Wahlgren, Chem. Phys. 244 (1999) 195.
[45] V. Vallet, B. Schimmelpfennig, L. Maron, C. Teichteil, T. Leininger, O. Gropen, I. Grenthe, U. Wahlgren, Chem. Phys. 244 (1999) 185.
[46] V. Vallet, L. Maron, B. Schimmelpfennig, T. Leininger, C. Teichteil, O. Gropen, I. Grenthe, U. Wahlgren, J. Phys. Chem. A 103 (1999) 9285.
[47] L. Gagliardi, C.-K Skylaris, A. Willetts, J.M. Dyke, V. Barone, Phys. Chem. Chem. Phys. 2 (2000) 3111.
[48] L. Gagliardi, B.O. Roos, Chem. Phys. Lett. 331 (2000) 229.
[49] Y.-K. Han, K. Hirao, J. Chem. Phys. 113 (2000) 7345.
[50] Y.-K. Han, J. Comput. Chem. 22 (2001) 2010.
[51] L. Joubert, P. Maldivi, J. Phys. Chem. A 105 (2001) 9068.
[52] V. Vallet, U. Wahlgren, B. Schimmelpfennig, H. Moll, Z. Zabo, I. Grenthe, Inorg. Chem. 40 (2001) 3516.
[53] M. García-Hernández, C. Lauterbach, S. Krüger, A. Matveev, N. Rösch, J. Comput. Chem. 23 (2002) 834.
[54] B.O. Roos, P.-O. Widmark, L. Gagliardi, Faraday Discuss. 124 (2003) 57.
[55] V. Vetere, P. Maldivi, C. Adamo, J. Comput. Chem. 24 (2003) 850.
[56] V. Vallet, U. Wahlgren, I. Grenthe, J. Am. Chem. Soc. 125 (2003) 14941.
[57] L. Andrews, B. Liang, J. Li, B.E. Bursten, New J. Chem. 28 (2004) 289.
[58] D. Guillaumont, J. Phys. Chem. A 108 (2004) 6893.
[59] V. Vetere, B.O. Roos, P. Maldivi, C. Adamo, Chem. Phys. Lett. 396 (2004) 452.
[60] C. Clavaguéra-Sarrio, N. Ismail, C.J. Marsden, D. Bégué, C. Pouchan, Chem. Phys. 302 (2004) 1.
[61] C. Clavaguéra-Sarrio, V. Vallet, D. Maynau, C.J. Marsden, J. Chem. Phys. 121 (2004) 5312.
[62] B. Liang, L. Andrews, J. Li, Inorg. Chem. 43 (2004) 882.
[63] E.R. Batista, R.L. Martin, P.J. Hay, J.E. Peralta, G.E. Scuseria, J. Chem. Phys. 121 (2004) 2144.
[64] E.R. Batista, R.L. Martin, P.J. Hay, J. Chem. Phys. 121 (2004) 11104.
[65] T. Privalov, P. Macak, B. Schimmelpfennig, E. Fromager, I. Grenthe, U. Wahlgren, J. Am. Chem. Soc. 126 (2004) 9801.
[66] P. Macak, E. Fromager, T. Privalov, B. Schimmelpfennig, I. Grenthe, U. Wahlgren, J. Phys. Chem. A 109 (2005) 4950.
[67] E. Fromager, V. Vallet, B. Schimmelpfennig, P. Macak, T. Privalov, U. Wahlgren, J. Phys. Chem. A 109 (2005) 4957.
[68] M. Straka, M. Kaupp, Chem. Phys. 311 (2005) 45.
[69] M. Straka, P. Hrobarik, M. Kaupp, J. Am. Chem. Soc. 127 (2005) 2591.
[70] X. Cao, Q. Li, A. Moritz, Z. Xie, M. Dolg, X. Chen, W. Fang, Inorg. Chem. (2006), in press.
[71] Y. Mochizuki, H. Tatewaki, Chem. Phys. 273 (2001) 135.